10-22-2020

Spatial Fingerprint of Younger Dryas Cooling and Warming in Eastern North America

David Fastovich

James M. Russell

Stephen T. Jackson

Teresa R. Krause

Shaun A. Marcott

See next page for additional authors

Authors

David Fastovich, James M. Russell, Stephen T. Jackson, Teresa R. Krause, Shaun A. Marcott, and John W. Williams

Geophysical Research Letters

RESEARCH LETTER
10.1029/2020GL090031

Spatial Fingerprint of Younger Dryas Cooling and Warming in Eastern North America

David Fastovich[1], James M. Russell[2], Stephen T. Jackson[3], Teresa R. Krause[3,4], Shaun A. Marcott[5], and John W. Williams[1,6]

[1]Department of Geography, University of Wisconsin-Madison, Madison WI, USA, [2]Department of Earth, Environmental, and Planetary Sciences, Brown University, Providence, RI, USA, [3]U.S. Geological Survey, Department of the Interior Southwest Climate Science Center, and Department of Geosciences, University of Arizona, Tucson, AZ, USA, [4]Department of Biology, Augsburg University, Minneapolis, MN, USA, [5]Department of Geoscience, University of Wisconsin-Madison, Madison, WI, USA, [6]Center for Climatic Research, University of Wisconsin-Madison, Madison, WI, USA

Abstract The Younger Dryas (YD, 12.9–11.7 ka) is the most recent, near-global interval of abrupt climate change with rates similar to modern global warming. Understanding the causes and biodiversity effects of YD climate changes requires determining the spatial fingerprints of past temperature changes. Here we build pollen-based and branched glycerol dialkyl glycerol tetraether-based temperature reconstructions in eastern North America (ENA) to better understand deglacial temperature evolution. YD cooling was pronounced in the northeastern United States and muted in the north central United States. Florida sites warmed during the YD, while other southeastern sites maintained a relatively stable climate. This fingerprint is consistent with an intensified subtropical high during the YD and demonstrates that interhemispheric responses were more complex spatially in ENA than predicted by the bipolar seesaw model. Reduced-amplitude or antiphased millennial-scale temperature variability in the southeastern United States may support regional hotspots of biodiversity and endemism.

Plain Language Summary The Younger Dryas, circa 12,900 to 11,700 years ago, is a hemispheric abrupt climate change event that occurred at rates similar to those projected by the 21st century. Its cause has been linked to a reduction in northward oceanic heat transport in the Atlantic that led to Northern Hemispheric cooling and Southern Hemispheric warming. Here we present detailed reconstructions of Younger Dryas temperature variations in eastern North America that suggest a more complex spatial fingerprint than predicted by the standard global model. New England, Maritime Canada, and the Great Lakes Region all cooled, like Greenland and elsewhere in the Northern Hemisphere. However, regions south of Virginia experienced little temperature change and Florida warmed slightly. Possible mechanisms include atmospheric processes that enhanced advection from the subtropics and oceanic processes that transported heat northward from the equatorial Atlantic. These reconstructions also help explain the hotspot of biodiversity and endemic species in the southeastern United States, by showing that this region was buffered from past abrupt millennial-scale climate reversals.

Key Points:
- The spatial fingerprint of Younger Dryas (YD) temperature changes is reconstructed in eastern North America from brGDGTs and fossil pollen
- Reconstructions demonstrate higher YD temperatures in Florida, no change south of 40°N, and cooling north of 40°N
- These patterns are consistent with intensified subtropical highs during the YD and help explain high regional biodiversity

Supporting Information:
- Supporting Information S1

Correspondence to:
D. Fastovich,
fastovich@wisc.edu

Citation:
Fastovich, D., Russell, J. M., Jackson, S. T., Krause, T. R., Marcott, S. A., & Williams, J. W. (2020). Spatia l fingerprint of Younger Dryas cooling and warming in eastern North America. *Geophysical Research Letters*, *47*, e2020GL090031. https://doi.org/10.1029/2020GL090031

Received 24 JUL 2020
Accepted 15 OCT 2020
Accepted article online 22 OCT 2020

Author Contributions:
Conceptualization: David Fastovich, John W. Williams
Formal analysis: David Fastovich, James M. Russell, Stephen T. Jackson, Teresa R. Krause, Shaun A. Marcott, John W. Williams
Methodology: David Fastovich, James M. Russell, John W. Williams
Writing - original draft: David Fastovich
Writing – review & editing: David Fastovich, James M. Russell, Stephen T. Jackson, Teresa R. Krause, Shaun A. Marcott, John W. Williams

1. Introduction

The most recent deglaciation, 19.0 to 8.2 ka BP, contained several large hemispheric- to global-scale abrupt temperature changes with rates that are regionally comparable to projected 21st century climate change (Williams & Burke, 2019). Such millennial-scale climate variability profoundly affected vegetation and megafauna in Europe (Cooper et al., 2015; Huntley et al., 2013; Rey et al., 2017). In particular, the Younger Dryas (YD), dated to 12.9 to 11.7 ka (Rasmussen et al., 2006), is recorded in many Northern Hemispheric records (Clark et al., 2012) as a return to cold conditions. This cooling is attributed to a weakening of the Atlantic Meridional Overturning Circulation (AMOC) (Keigwin et al., 1991), causing a southward shift of the Intertropical Convergence Zone and weakened Northern Hemisphere monsoons (Kageyama et al., 2013; Talbot et al., 2007). The canonical bipolar seesaw hypothesis predicts that the YD and other stadials were caused by AMOC slowdown and reduced interhemispheric heat transport (Stocker, 1998). Prior global-scale data syntheses (Shakun & Carlson, 2010) and freshwater hosing experiments with climate models of varying complexity (Kageyama et al., 2013; Stocker et al., 1992) have shown

hemispheric-scale fingerprints (Northern Hemisphere cooling and Southern Hemisphere warming) consistent with the bipolar seesaw. Earth System Models (ESMs) predict more complex intrahemispheric fingerprints of temperature variations (Kageyama et al., 2013; Liu et al., 2009; Okumura et al., 2009), but these simulations remain poorly constrained by proxy data. This data gap limits our understanding of the mechanisms of heat redistribution following rapid changes in the AMOC (Pedro et al., 2018) and how biodiversity hotspots persisted during abrupt millennial-scale climate variations (Brown et al., 2020).

Eastern North America (east of 92°W) (ENA) has a dense network of paleoclimatic proxy records (Bartlein et al., 2011; Kaufman et al., 2020) and is a classic region for data-model comparisons (COHMAP Members, 1988). Earlier proxy-data syntheses of YD temperature variations in ENA are hampered by inaccuracies in conventional bulk-sediment radiocarbon dates (Grimm et al., 2009; Shuman et al., 2002) and prior global proxy syntheses for the YD emphasized marine records with few or no terrestrial ENA paleoclimatic records (Clark et al., 2012; Shakun & Carlson, 2010). A comparison of hosing experiments indicates that ENA is an area of high divergence among ESMs, with some predicting that ENA follows Northern Hemisphere cooling trends and others indicating no change or even regional warming (Kageyama et al., 2013). These differences among models for ENA result from uncertainty about the atmospheric and oceanic teleconnections by which the AMOC signal propagates from the North Atlantic.

Within ENA, the southeastern United States (between 30°N and 39°N) (SEUS) is climatically and biologically distinct. For example, a "warming hole" during the 20th and 21st century in the SEUS may be linked to decadal variability in the North Atlantic (Kumar et al., 2013) or the Pacific (Meehl et al., 2012). Climatic variations associated with the North Atlantic Oscillation (NAO) cause antiphased warm and dry/cool and wet climate anomalies in the SEUS and northeastern United States (Hurrell et al., 2003)—a climatic dipole that might affect past climate changes. The SEUS is a biodiversity hotspot, with high richness and endemism in amphibians, birds, reptiles, and plants (Jenkins et al., 2015). Climate stability during glacial-interglacial variations is one proposed mechanism for contemporary biodiversity and endemism (Brown et al., 2020; Sandel et al., 2011), but millennial-climate variability in the SEUS is largely unexplored.

Here, we present new reconstructions and syntheses of the deglacial temperature evolution in ENA, drawing upon a network of well-dated lacustrine multiproxy records and nearby marine records. We reconstruct mean annual temperatures from fossil pollen and branched glycerol dialkyl glycerol tetraethers (brGDGT) from sites spanning a 21.5° latitudinal gradient. We combine recently published brGDGT and pollen records from Bonnett Lake, OH (Fastovich et al., 2020), Silver Lake, OH (Watson et al., 2018), and White Pond, SC (Krause et al., 2019) with two new brGDGT records from Sheelar Lake, FL, Cupola Pond, MO, 42 well-dated pollen records from the Neotoma Paleoecology Database (Williams et al., 2018), and three nearby marine records of sea surface temperatures (SSTs) and storminess (Carlson et al., 2008; Toomey et al., 2017; Ziegler et al., 2008) (Figure S1 in the supporting information). We discuss the implications of the reported patterns for understanding mechanisms of deglacial climate evolution and contemporary patterns of biodiversity.

2. Methods

2.1. Site Selection and Age-Depth Modeling

Fossil pollen records and geochronological controls were obtained from the Neotoma Paleoecology Database (Goring et al., 2015; Williams et al., 2018). We performed an initial search for all sites east of 92°W, including several sites recently contributed by the authors of this study (Fastovich et al., 2020; Krause et al., 2019; Watson et al., 2018). As a second-pass filter, we used all fossil pollen records according to the following chronological and sampling criteria: (i) two or more chronological controls in the record, (ii) one or more chronological controls from 15.5 to 10.9 ka, and (iii) at least four pollen samples from 13.8 to 11.1 ka. When setting these criteria, we sought to balance a tradeoff between minimizing temporal uncertainty and maximizing spatial coverage. We used 42 records for the late-glacial spatial fingerprint analyses, of which 27 extended to 15.5 ka and so were included in the principal components analysis (PCA) (Table S1 and Figure S1). New age-depth relationships were built using *Bacon* (Blaauw & Christen, 2011) and *bulk baconizing* (Wang et al., 2019).

2.2. Mean Annual Temperature Reconstructions

brGDGTs are a class of lipids found in bacterial membranes; the relative abundances of brGDGTs is sensitive to environmental factors such as temperature and pH (Weijers et al., 2007). We analyzed existing sediments from Cupola Pond, MO (Jones et al., 2017), and a new core from Sheelar Lake, FL (Figure S2 and Table S2) for brGDGTs. Previous publications on sediment cores from White Pond and Silver Lake used a then-current chromatographic method, in which 5- and 6-methyl isomers co-elute (Weijers et al., 2007). At the three sites analyzed more recently (Bonnett Lake, Cupola Pond, & Sheelar Lake), an updated approach was used that separates 5- and 6-methyl brGDGT isomers (Hopmans et al., 2016) and allows for more precise temperature calibrations (De Jonge et al., 2014). At Silver Lake, we compared the two analytical approaches by reanalyzing a subset of the original samples using the updated method and found similar temperature reconstructions (Figure S3) (Fastovich et al., 2020). We reconstructed mean annual temperature using the MAT MBT'_{5Me} calibration function for sites where 5- and 6-methyl isomers were separated (De Jonge et al., 2014), and the Peterse et al. (2012) calibration at White Pond (Krause et al., 2019) and Silver Lake (Watson et al., 2018), which are based on the calibration of brGDGTs in soil samples to temperature. These calibrations were selected because they more accurately reconstruct modern mean annual temperature than calibrations built from east African lake sediment samples (e.g., Russell et al., 2018) (Figure S4) and the MBT'_{5Me} and MBT' index quantify brGDGT methylation, which is hypothesized to control membrane fluidity (Sinninghe Damsté et al., 2018). Microbial community composition also affects the abundances of brGDGT molecules (De Jonge et al., 2019).

Errors were calculated using an ensemble of bootstrapped calibration parameters (Loomis et al., 2012) trained on calibration data from Peterse et al. (2012) and De Jonge et al. (2014) to estimate the 95% confidence interval for temperature estimates. The effect of temporal uncertainty was incorporated by creating randomly sampled pairs of bootstrapped temperature estimates with a draw from the posterior age distribution for each brGDGT sample. These pairs were then interpolated onto an even 100-year interval, generating an ensemble of linearly interpolated temperature estimates for each site.

Pollen-inferred mean annual temperature reconstructions were averaged across three transfer functions: modern analog technique (Overpeck et al., 1985), weighted averaging (Ter Braak, 1987; Ter Braak & Prentice, 1988), and weighted-average partial least squares (Ter Braak et al., 1993; Ter Braak & Juggins, 1993). The transfer functions were trained on modern pollen abundances from the North American Modern Pollen Database (NAMPD) (Whitmore et al., 2005). Pollen abundances in the modern calibration data set and the fossil pollen were aggregated into 64 taxa (Williams & Shuman, 2008). Following Williams and Shuman (2008), taxonomic ambiguity in the NAMPD was addressed by geographically splitting *Picea* into eastern and western types, *Pinus* into northeastern and southeastern types, and Myricaceae into northern and southern types, to reduce the possibility of false matches, using species maps from Thompson et al. (1999a, 1999b). A more detailed procedure was followed for the fossil pollen taxa. All sites in Florida were assumed to consist of southeastern *Pinus* (many species), while all sites above 40°N were assumed to consist of northeastern *Pinus* (*P. banksiana*, *P. resinosa*, & *P. strobus*), for the entirety of the records (Jackson et al., 1997, 2000). Sites between Florida and 40°N demonstrate a clear temporal separation between the decline of northeastern *Pinus* and the establishment of southeastern *Pinus* (e.g., White Pond, SC; Krause et al., 2019). Pollen size analyses of *Pinus* at White Pond supports this delineation between northeastern and southeastern *Pinus* (Watts, 1980b). At these sites, the earlier period of high *Pinus* abundances was assumed to represent northeastern species and the second period of high abundances was assumed to be southeastern (Table S3). *Picea* was assumed to be eastern and all fossil and modern instances of Myricaceae were split into northern and southern populations at 35 °N (Williams et al., 2006). After generating temperature estimates, fossil pollen temperatures were interpolated onto an even 100-year interval, regionally averaged to produce regional time series, and spatially averaged into 2° bins.

2.3. Spatial Analysis of Temperature Reconstructions

PCA of the temperature time series was performed to determine common modes of variation in the temperature reconstructions (Mix et al., 1986a, 1986b; Shakun & Carlson, 2010). We also included prior SST reconstructions from Blake Outer Ridge (Carlson et al., 2008) and MD02-2575 (Ziegler et al., 2008) in the PCA. The effect of temporal uncertainty on the PCA was included by creating an ensemble of interpolated temperature estimates for each site, based on randomly selected posterior age estimates. PCA was performed 10,000 times

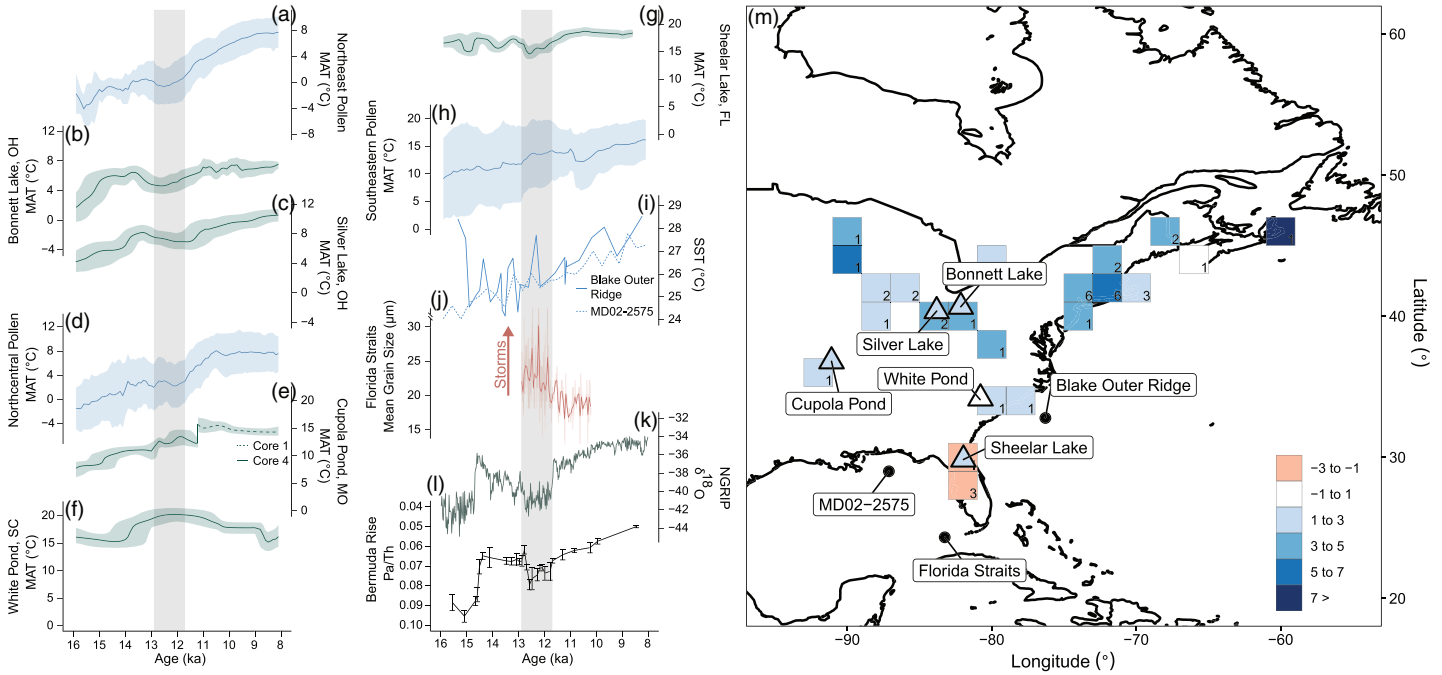

Figure 1. (a, d, and h) Regionally averaged reconstructions of mean annual temperatures for the northeastern (a), north central (d), and southeastern United States (h) based on fossil pollen ensembles. Shading indicates 1-σ intersite standard deviation. (b, c, and e–g) brGDGT-inferred temperatures with the single-site 95% confidence interval. (i) Mg/Ca sea surface temperatures (Carlson et al., 2008; Ziegler et al., 2008). (j) Mean grain size for core KNR166–2 JPC25 near the Florida Straits as a proxy for hurricane activity (Toomey et al., 2017) with the light red line indicating the raw data and dark red line indicating a 50-year moving mean. (k) $\delta^{18}O$ oxygen isotopes from NGRIP (Rasmussen et al., 2006). (l) AMOC strength, based on Pa/Th ratio (McManus et al., 2004). Gray column indicates the Younger Dryas Interval. (m) Temperature differences (°C) from the mid-Younger Dryas (YD, 12.3 ka) to the early Holocene (EH, 11.1 ka) based on brGDGT (triangles) and pollen (grid cells). Anomalies are expressed as EH-YD and color coded so that blue indicates a cooler YD and red a warmer YD. The number of pollen records is indicated in each grid cell. Other sites from Figure 1 are indicated as black dots.

on matrices composed of a randomly sampled temperature ensemble member from each site. The SST records had only point age estimates, with no uncertainties, so these records were incorporated unchanged in all PCA replicates. Although age was not varied in the SST records, sensitivity experiments indicated this had little impact on the uncertainty estimates of the PC time series values (<0.023). All random sampling was performed assuming a uniform distribution, thus equally weighing ensemble members of age and temperature estimates. The 95% high-density interval of the principal components was retained, producing the median and confidence interval in Figure 2. We assessed the significance of the PCs in all ensemble members using broken-stick significance testing (Jackson, 1993) and the North et al. (1982) uniqueness test (Figure S5). PC1 and PC2 explained 58% (95% CI: 44%, 78%) and 16% (95% CI: 11%, 23%) of the variance, respectively. PC1 was significant in all ensemble members using the broken-stick test and unique in all of the ensemble members using the North et al. (1982) "rule of thumb" (Figure S5). PC2 was significant in almost all ensemble members (broken-stick test) and unique in 27% of the ensemble members (Figure S5).

3. Results

3.1. YD Temperatures

Deglacial temperature evolution in ENA exhibits a coherent spatial fingerprint with at least three distinct modes (Figures 1 and 2). The northeast cooled during YD onset (1.0°C), with similar timing to Greenland (Rasmussen et al., 2006), and is signaled by the rapid resurgence of boreal plant taxa (Figures 1a and 1m) and chironomid indicators (Levesque et al., 1997). Pollen and brGDGT temperature estimates in the north central United States also indicate YD cooling, but with a possibly lagged onset of ~400 years (0.9–2.0°C; Figures 1b–1d). This apparent lag may be due to regional climatic processes, such as local ice sheet effects on atmospheric circulation (see Gonzales & Grimm, 2009), that overprint AMOC-induced cooling.

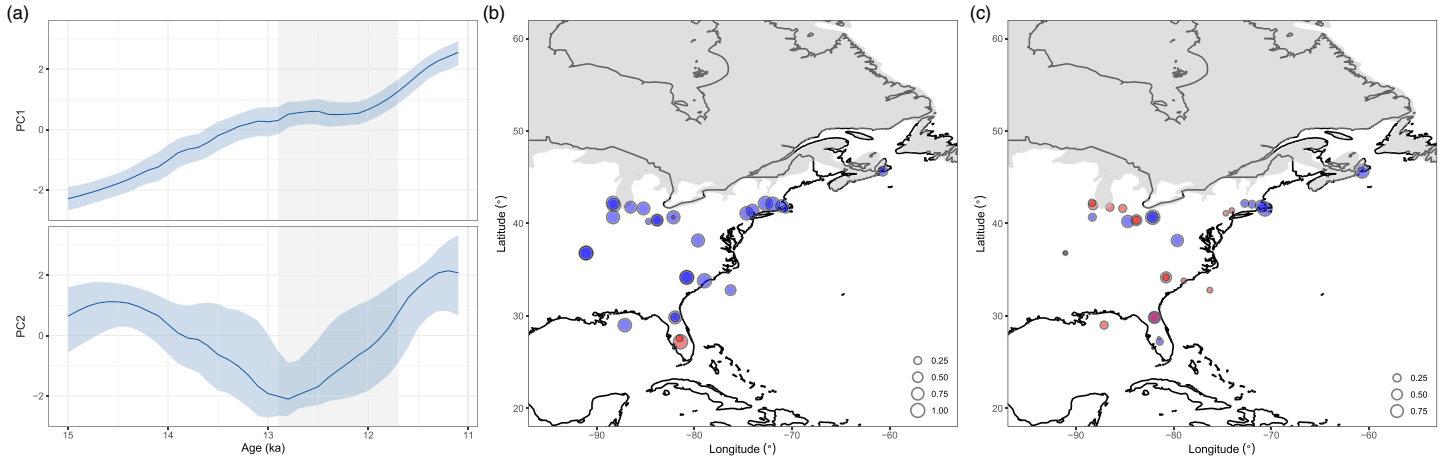

Figure 2. (a) Time series of PC1 and PC2 for all temperature records that extended through the interval of 15 to 11.1 ka. Shading indicates 95% confidence interval. (b) PC1 and (c) PC2 loadings, with blue indicating positive and red indicating negative loadings. Gray outline represents the extent of the Laurentide Ice Sheet at 12,000 ^{14}C years (Dyke et al., 2003).

Overall, sites closer to the North Atlantic cooled more (Figure 1m), indicating the sensitivity of northeastern sites to reduced AMOC or greater regional sea ice extent, which would have produced albedo feedbacks and increased cooling (Gildor & Tziperman, 2001; North, 1984). Additionally, our analysis compares YD temperatures to early Holocene temperatures, and regions adjacent to the Laurentide Ice Sheet likely experienced a greater deglacial to Holocene warming (Tierney et al., 2020).

In contrast, in the SEUS, temperatures were stable or rising during the YD and, in Florida, were warmer than during the early Holocene (Figures 1e–1h and 1m). All pollen-based paleoclimatic reconstructions indicate SEUS warming during the YD, which is supported by the replacement of boreal conifers (*Picea, Pinus*) with temperate conifers (*Tsuga*) at 38.2°N (Kneller & Peteet, 1993) and temperate hardwoods (*Quercus, Carya, Ostrya/Carpinus*, and *Corylus*) at 36.8°N (Jones et al., 2017). Two of the three southern brGDGT records agree with the pollen-based temperature reconstructions, with Cupola and White Ponds showing no YD cooling, but Sheelar Lake indicates a cooling (<3°C). Despite this disagreement, pollen- and brGDGT-inferred temperatures produce a coherent spatial pattern that discriminates the SEUS and northern sites. PC1, which tracks deglacial warming (Figure 2a), shows strong positive loadings for northern sites and strong negative loadings for central Florida (Figure 2b). PC2, which tracks YD cooling (Figure 2a), shows a strong signal in the northeastern United States, a variable loading magnitude and sign in the upper Midwest, and a weak signal in the SEUS, where 8 of 12 records having loadings <0.25 (Figure 2c). Small negative loadings in the SEUS indicates that these sites contribute less to PC2 and are negatively correlated with PC2. This suggests that most sites in the SEUS experienced slight warming through the YD, rather than the large cooling inferred from the large positive loadings in the northern regions. As a result, the ENA temperature gradient weakens after 13 ka, with a pause or slight reversal during the YD (Figure S6). These analyses suggest that temperature variations were muted in SEUS during the YD, particularly between 30°N to 35°N (Figures 1m and S6). Above 35°N, temperature trends resemble the millennial-scale variations seen in temperature records from the North Atlantic and Greenland (Shakun & Carlson, 2010) (Figures 1, 2, and S7–S9).

This temperature fingerprint is consistent with nearby marine records (Figures 1i and 2) and helps resolve putative outliers in prior global syntheses (Shakun & Carlson, 2010). North Atlantic marine records show YD cooling (Bard et al., 2000), similar to the temperature trends for the northeastern and north central United States (Figure 1 and S7–S9). SSTs at Blake Outer Ridge (32°47′N), in contrast, demonstrate gradual YD warming (Figure 1i) (Carlson et al., 2008). SST estimates from the northeast Gulf of Mexico (Figure 1i) (Ziegler et al., 2008) and northern Caribbean (Ruhlemann et al., 1999) also exhibit YD warming and no abrupt onset. Cyclone frequency or intensity in the subtropical Atlantic increased during the YD, consistent with regionally elevated SSTs or lower-amplitude cooling than elsewhere in the Atlantic (Figure 1j) (Toomey et al., 2017). Hence, the spatial fingerprint apparent in terrestrial ENA may have also manifested in the adjacent subtropical Atlantic and Gulf of Mexico.

4. Discussion

4.1. Mechanisms for Regionally Varying YD Temperatures

Global climate model (GCM) experiments and the modern climatology of ENA identify several plausible mechanisms for the spatial fingerprint of YD climate change in ENA. One working hypothesis is an enhanced subtropical high that resembles the positive phase of the NAO. The NAO is associated with gradients in mean atmospheric pressure in the North Atlantic and subtropics, and influences temperature and precipitation in ENA through changes in the mean position of the jet stream and westerlies (Walker & Bliss, 1932; Wallace & Gutzler, 1981) (Figure 3). Boreal winters with a large positive index (greater difference in pressure between the Icelandic Low and Azores High) are associated with a stronger and more zonal jet (Bjerknes, 1964), shifting storm tracks northward (Rogers, 1990). This jet stream configuration produces southerly flow into SEUS and higher temperatures (Deser & Blackmon, 1993; Walker & Bliss, 1932), and northeasterly flow into the northeastern and north central United States, producing colder winters (Hurrell et al., 2003). NAO-positive years also correlate with increased tropical storm activity (Elsner & Kocher, 2000). These patterns are consistent with the observed spatial fingerprint (Figures 1 and 2), with records of tropical storm activity during the YD (Toomey et al., 2017) (Figure 1j), and with pollen-based interpretations of a wet YD in Florida (Grimm et al., 2006). Several paleoclimatic records in Europe that span the YD demonstrate a repositioning and strengthening of westerly winds and support our finding for NAO positive conditions (Baldini et al., 2015; Brauer et al., 2008). Furthermore, GCM experiments with a freshwater forcing simulate anomalously high pressure near the Azores (Ivanovic et al., 2017; Renssen et al., 2018). Notably, colder SSTs in the North Atlantic are associated with a more positive NAO index caused by a deepening of the Icelandic Low (Bjerknes, 1964; van Loon & Rogers, 1978), which suggests that AMOC shutdown may have deepened the Icelandic Low, initiating an NAO-positive climate state. The initiation of NAO-positive conditions can be forced by SST anomalies in the North Atlantic due to changes to latent heat exchange from the ocean to atmosphere (Rodwell et al., 1999).

Positive NAO conditions are also associated with higher pressures in the subtropics and enhanced Hadley cell circulation and trade winds (Wang, 2002). An enhanced subtropical high may have also strengthened surface ocean circulation, drawing heat northward from the equatorial Atlantic. GCMs and proxies demonstrate a southward shift of the Hadley cell and strengthened trade winds following AMOC shutdown (McGee et al., 2018). These in turn may have enhanced easterly wind stress in the northern tropical Atlantic and the strength of the subtropical oceanic cell (McCreary & Lu, 1994), along with the meridional heat transport associated with the cell (Klinger & Marotzke, 2000). Increased heat transport by the subtropical cell could further intensify warming associated with southerly atmospheric advection into the SEUS due to NAO-positive conditions. A strengthening of the northern subtropical cell has been simulated in the Climate Model 2.1 GCM following hosing (Chang et al., 2008). Experiments with an Earth-system model of intermediate complexity suggest that warm SSTs in the Gulf of Mexico are necessary to producing warmer and wetter conditions in Florida following AMOC shutdown (Donders et al., 2011).

Other climatic influences may have also contributed to a warm SEUS. Paleoclimate reconstructions in the Gulf of Mexico suggest the presence of an enlarged Atlantic Warm Pool (Ziegler et al., 2008). Atmospheric circulation changes associated with the melting of the Laurentide Ice Sheet (Gregoire et al., 2015) also may have contributed to SEUS warming during the YD. Further work with ESMs is needed to better understand and test the potential contributions of these mechanisms to SEUS warming during the YD and other periods of enhanced freshwater forcing and AMOC weakening.

4.2. Biogeographic Implications of a Warm YD

The SEUS is a biodiversity hotspot for multiple taxonomic groups (Jenkins et al., 2015), and the muted YD temperature change we document in the SEUS suggest a mechanism for maintaining regional biological diversity. Various explanations have been offered for the higher species richness and endemism in ENA than Europe, including different configurations of climate refugia and mountain barriers to species migration, and differing amplitudes of glacial-interglacial climate change (Latham & Ricklefs, 1993; Lumibao et al., 2017; Sandel et al., 2011). Other papers have linked the global distribution of biodiversity hotspots to Quaternary climate stability without disentangling orbital and millennial components (Brown et al., 2020). Our work suggests that the high climate stability in the SEUS during past abrupt millennial-scale climate changes may have uniquely positioned the SEUS to be a biodiversity preserve. This contrasts with western

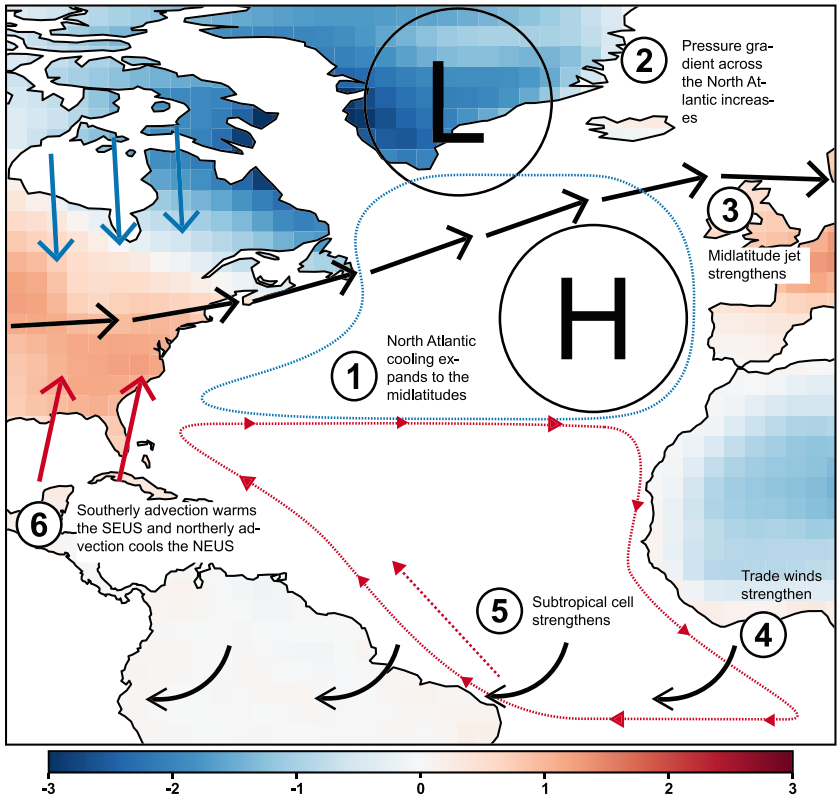

Figure 3. Schematic of hypothesized mechanisms for SEUS YD warming and observed temperature fingerprint. Shading corresponds to the slope of a regression of surface temperature on the NAO index (Hurrell, 1995) from the NCEP Reanalysis data product (Kalnay et al., 1996). Positive slope indicates positive correlation of surface temperature to the NAO index. Solid lines indicate atmospheric processes and dashed lines indicate oceanic processes.

Eurasia, which experienced high-amplitude millennial-scale climate variability, megafaunal turnover (Cooper et al., 2015), and forest losses during stadials, partially due to its exposed position downwind of the North Atlantic (Huntley et al., 2013). This hypothesis does not exclude other hypotheses for the differential biodiversity in the SEUS and Europe (e.g., mountain barriers), but low millennial-scale climatic variability may be a potentially important mechanism for maintaining climatic stability and facilitating biodiversity persistence.

4.3. Caveats and Uncertainties

Our temperature inferences are subject to various uncertainties, but these can be minimized and do not affect the general conclusions. Temporal uncertainty was reduced by using sites with multiple chronological controls near the period of interest. Moreover, 37 of the 42 sites used in the spatial analysis of temperature change have seven or more chronologic controls with several sites in each region containing 10 or more controls (Table S1). When the effect of temporal uncertainty on early Holocene and mid-YD anomalies is assessed, the SEUS remains climatologically distinct from the other two regions (Figure S10).

Ambiguity in *Pinus* pollen can confound pollen-based temperature reconstructions because *Pinus* is a common pollen type and the genus contains 13 species in ENA distributed from Florida to Canada. We have minimized this bias by splitting *Pinus* pollen into northern and southern types (Williams & Shuman, 2008) in the modern calibration dataset and fossil pollen data set. Lastly, deglacial vegetation dynamics (and fossil pollen records) were governed by multiple climate variables such as moisture availability, growing degree days, and winter severity. We have focused on mean annual temperature, while acknowledging these other effects. The multivariate transfer functions used here are designed to extract multiple climatic signals from fossil assemblages (Overpeck et al., 1985; Ter Braak, 1987; Ter Braak et al., 1993; Ter Braak & Juggins, 1993; Ter Braak & Prentice, 1988) and the independent temperature reconstructions

from brGDGTs agree well with fossil pollen reconstructions of mean annual temperature (Fastovich et al., 2020; Watson et al., 2018) (Figure 1). Moreover, PCA as a multivariate method helps deconvolve multiple climatic signals and other controls on fossil pollen abundance.

The brGDGT temperature estimates also contain uncertainties, largely sourced from calibration data sets, but the qualitative temperature trends inferred from brGDGTs are robust, given the small measurement error, as long as MBT values depend on temperature (Sinninghe Damsté et al., 2018). Various factors contribute to these uncertainties. Differences in brGDGT distributions between soils and lake sediments can add uncertainty to temperature estimates, if sediment provenance and brGDGT sources change over time. The use of soil-based brGDGT in our study sites is supported by accurate reconstructions of modern mean annual temperature at all sites (Figure S4) and accurate reconstructions of soil pH at Bonnett Lake, Silver Lake, and White Pond (Fastovich et al., 2020; Krause et al., 2019; Watson et al., 2018). Seasonality in midlatitudinal sites has also recently been identified as a source of error in brGDGT temperature calibrations (Crampton-Flood et al., 2020). One or several of these various uncertainties may be relevant at Sheelar Lake, where the brGDGT temperature reconstruction disagrees with the pollen-based reconstructions and other nearby brGDGT reconstructions. Despite these uncertainties, the consistency in pattern across multiple independent terrestrial and marine proxies strongly supports the spatial fingerprint reported here.

5. Conclusions

Our multiproxy fingerprint analysis of YD temperatures in ENA suggests at least three distinct regional climate histories, consistent with shifts in AMOC and atmospheric heat transport. Florida and the SEUS warmed during the YD, with nearby marine records indicating YD warming and intensified storminess (Carlson et al., 2008; Toomey et al., 2017). The northeastern United States resembles Greenland in timing of cooling while cooling in the north central United States was dampened and with a possible lagged onset. These patterns suggest higher climate stability between 30°N and 35°N and support a more complex model of YD climate change than suggested by the standard bipolar seesaw. AMOC shutdown may have caused local warming in the SEUS through dynamical changes to atmospheric circulation induced by NAO positive conditions or changes in the strength of the subtropical cell. Further analysis using ESMs under hosing conditions is necessary to constrain the relevant mechanisms. Dampened millennial-scale climate variability in the SEUS may have helped enhance regional climate stability thereby preserving regional biodiversity.

Data Availability Statement

Fossil pollen counts and brGDGT proportions can be accessed from the Neotoma Paleoecology Database using the Neotoma API (http://api.neotomadb.org/api-docs) or the *get_download* function of the *neotoma* R-package, and the Site ID or Dataset ID from Table S1. The Site ID returns all data available for a site and the Dataset ID returns the pollen abundances used in this study for a single site.

Acknowledgments

We thank E. C. Grimm for providing Lake Annie fossil pollen data, Laura Messier for assistance in brGDGT analysis, and Connor Nolan for field assistance. We also thank Jeremiah Marsicek for assistance in quantifying temporal uncertainty in brGDGT records. This work was supported by the National Science Foundation (DEB-1353896 and DEB-1349662). Reviews from Bronwen Konecky and four anonymous reviewers greatly improved the manuscript. Any use of trade, firm, or product name is for descriptive purposes and does not imply endorsement by the U.S. Government.

References

Baldini, L. M., McDermott, F., Baldini, J. U. L., Arias, P., Cueto, M., Fairchild, I. J., et al. (2015). Regional temperature, atmospheric circulation, and sea-ice variability within the Younger Dryas Event constrained using a speleothem from northern Iberia. *Earth and Planetary Science Letters*, *419*, 101–110. https://doi.org/10.1016/j.epsl.2015.03.015

Bard, E., Rostek, F., Turon, J. L., & Gendreau, S. (2000). Hydrological impact of Heinrich events in the subtropical northeast Atlantic. *Science*, *289*(5483), 1321–1324. https://doi.org/10.1126/science.289.5483.1321

Bartlein, P. J., Harrison, S. P., Brewer, S., Connor, S., Davis, B. A. S., Gajewski, K., et al. (2011). Pollen-based continental climate reconstructions at 6 and 21 ka: A global synthesis. *Climate Dynamics*, *37*(3–4), 775–802. https://doi.org/10.1007/s00382-010-0904-1

Bjerknes, J. (1964). Atlantic Air-Sea interaction. In H. E. Landsberg & J. Van Mieghem (Eds.), *Advances in Geophysics* (pp. 1–82). New York: Academic Press.

Blaauw, M., & Christen, J. A. (2011). Flexible paleoclimate age-depth models using an autoregressive gamma process. *Bayesian Analysis*, *6*(3), 457–474.

Brauer, A., Haug, G. H., Dulski, P., Sigman, D. M., & Negendank, J. F. W. (2008). An abrupt wind shift in western Europe at the onset of the Younger Dryas cold period. *Nature Geoscience*, *1*(8), 520–523.

Brown, S. C., Wigley, T. M. L., Otto-Bliesner, B. L., Rahbek, C., & Fordham, D. A. (2020). Persistent Quaternary climate refugia are hospices for biodiversity in the Anthropocene. *Nature Climate Change*, *10*(3), 244–248. https://doi.org/10.1038/s41558-019-0682-7

Carlson, A. E., Oppo, D. W., Came, R. E., LeGrande, A. N., Keigwin, L. D., & Curry, W. B. (2008). Subtropical Atlantic salinity variability and Atlantic meridional circulation during the last deglaciation. *Geology*, *36*(12), 991–994. https://doi.org/10.1130/G25080A.1

Chang, P., Zhang, R., Hazeleger, W., Wen, C., Wan, X. Q., Ji, L., et al. (2008). Oceanic link between abrupt changes in the North Atlantic Ocean and the African monsoon. *Nature Geoscience*, *1*(7), 444–448. https://doi.org/10.1038/ngeo218

Clark, P. U., Shakun, J. D., Baker, P. A., Bartlein, P. J., Brewer, S., Brook, E., et al. (2012). Global climate evolution during the last deglaciation. *Proceedings of the National Academy of Sciences*, *109*(19), E1134–E1142. https://doi.org/10.1073/pnas.1116619109

Cooper, A., Turney, C., Hughen, K. A., Brook, B. W., McDonald, H. G., & Bradshaw, C. J. A. (2015). Abrupt warming events drove late Pleistocene Holarctic megafaunal turnover. *Science*, *349*(6248), 602–606. https://doi.org/10.1126/science.aac4315

Cooperative Holocene Mapping Project Members (1988). Climatic changes of the last 18,000 years: Observations and model simulations. *Science*, *241*(4869), 1043–1052.

Crampton-Flood, E. D., Tierney, J. E., Peterse, F., Kirkels, F. M. S. A., & Damste, J. S. S. (2020). BayMBT: A Bayesian calibration model for branched glycerol dialkyl glycerol tetraethers in soils and peats. *Geochimica et Cosmochimica Acta*, *268*, 142–159. https://doi.org/10.1016/j.gca.2019.09.043

De Jonge, C., Hopmans, E. C., Zell, C. I., Kim, J.-H., Schouten, S., & Sinninghe Damsté, J. S. (2014). Occurrence and abundance of 6-methyl branched glycerol dialkyl glycerol tetraethers in soils: Implications for palaeoclimate reconstruction. *Geochimica et Cosmochimica Acta*, *141*(Supplement C), 97–112. https://doi.org/10.1016/j.gca.2014.06.013

De Jonge, C., Radujkovic, D., Sigurdsson, B. D., Weedon, J. T., Janssens, I., & Peterse, F. (2019). Lipid biomarker temperature proxy responds to abrupt shift in the bacterial community composition in geothermally heated soils. *Organic Geochemistry*, *137*, 13.

Deser, C., & Blackmon, M. L. (1993). Surface climate variations over the North Atlantic during the winter: 1900–1989. *Journal of Climate*, *6*(9), 1743–1753. https://doi.org/10.1175/1520-0442(1993)006<1743:SCVOTN>2.0.CO;2

Donders, T. H., de Boer, H. J., Finsinger, W., Grimm, E. C., Dekker, S. C., Reichart, G. J., & Wagner-Cremer, F. (2011). Impact of the Atlantic Warm Pool on precipitation and temperature in Florida during North Atlantic cold spells. *Climate Dynamics*, *36*(1–2), 109–118. https://doi.org/10.1007/s00382-009-0702-9

Dyke, A. S., Moore, A., & Robertson, L. (2003). Deglaciation of North America, in *Natural Resources Canada, Ottawa*, edited by O. F. Geological Survey of Canada.

Elsner, J. B., & Kocher, B. (2000). Global tropical cyclone activity: A link to the North Atlantic Oscillation. *Geophysical Research Letters*, *27*(1), 129–132. https://doi.org/10.1029/1999GL010893

Fastovich, D., Russell, J. M., Jackson, S. T., & Williams, J. W. (2020). Deglacial temperature controls on no-analog community establishment in the Great Lakes Region. *Quaternary Science Reviews*, *234*, 106245. https://doi.org/10.1016/j.quascirev.2020.106245

Gildor, H., & Tziperman, E. (2001). A sea ice climate switch mechanism for the 100-kyr glacial cycles. *Journal of Geophysical Research*, *106*(C5), 9117–9133. https://doi.org/10.1029/1999JC000120

Gonzales, L. M., & Grimm, E. C. (2009). Synchronization of late-glacial vegetation changes at Crystal Lake, Illinois, USA with the North Atlantic Event Stratigraphy. *Quaternary Research*, *72*(2), 234–245. https://doi.org/10.1016/j.yqres.2009.05.001

Goring, S., Dawson, A., Simpson, G., Ram, K., Graham, R., Grimm, E., & Williams, J. (2015). Neotoma: A programmatic interface to the Neotoma Paleoecological Database. *Open Quaternary*, *1*(1), 1–17. https://doi.org/10.5334/oq.ab

Gregoire, L. J., Valdes, P. J., & Payne, A. J. (2015). The relative contribution of orbital forcing and greenhouse gases to the North American deglaciation. *Geophysical Research Letters*, *42*, 9970–9979. https://doi.org/10.1002/2015GL066005

Grimm, E. C., Maher, L. J., & Nelson, D. M. (2009). The magnitude of error in conventional bulk-sediment radiocarbon dates from central North America. *Quaternary Research*, *72*(2), 301–308. https://doi.org/10.1016/j.yqres.2009.05.006

Grimm, E. C., Watts, W. A., Jacobson, G. L., Hansen, B. C. S., Almquist, H. R., & Dieffenbacher-Krall, A. C. (2006). Evidence for warm wet Heinrich events in Florida. *Quaternary Science Reviews*, *25*(17–18), 2197–2211. https://doi.org/10.1016/j.quascirev.2006.04.008

Hopmans, E. C., Schouten, S., & Sinninghe Damsté, J. S. (2016). The effect of improved chromatography on GDGT-based palaeoproxies. *Organic Geochemistry*, *93*, 1–6. https://doi.org/10.1016/j.orggeochem.2015.12.006

Huntley, B., Allen, J. R. M., Collingham, Y. C., Hickler, T., Lister, A. M., Singarayer, J., et al. (2013). Millennial climatic fluctuations are key to the structure of last glacial ecosystems. *PLoS ONE*, *8*(4), e61963. https://doi.org/10.1371/journal.pone.0061963

Hurrell, J. W. (1995). Decadal trends in the North Atlantic Oscillation: Regional temperatures and precipitation. *Science*, *269*(5224), 676–679. https://doi.org/10.1126/science.269.5224.676

Hurrell, J. W., Kushnir, Y., Ottersen, G., & Visbeck, M. (2003). An overview of the North Atlantic oscillation. *Geophysical Monograph-American Geophysical Union*, *134*, 1–36.

Ivanovic, R. F., Gregoire, L. J., Wickert, A. D., Valdes, P. J., & Burke, A. (2017). Collapse of the North American ice saddle 14,500 years ago caused widespread cooling and reduced ocean overturning circulation. *Geophysical Research Letters*, *44*, 383–392. https://doi.org/10.1002/2016GL071849

Jackson, D. A. (1993). Stopping rules in pricipal components analysis: A comparison of heuristical and statistical approaches. *Ecology*, *74*(8), 2204–2214. https://doi.org/10.2307/1939574

Jackson, S. T., Overpeck, J. T., Webb, T. III, Keattch, S. E., & Anderson, K. H. (1997). Mapped plant-macrofossil and pollen records of late quaternary vegetation change in Eastern North America. *Quaternary Science Reviews*, *16*(1), 1–70. https://doi.org/10.1016/s0277-3791(96)00047-9

Jackson, S. T., Webb, R. S., Anderson, K. H., Overpeck, J. T., Webb, T. III, Williams, J. W., & Hansen, B. C. S. (2000). Vegetation and environment in eastern North America during the Last Glacial Maximum. *Quaternary Science Reviews*, *19*(6), 489–508. https://doi.org/10.1016/S0277-3791(99)00093-1

Jenkins, C. N., Van Houtan, K. S., Pimm, S. L., & Sexton, J. O. (2015). US protected lands mismatch biodiversity priorities. *Proceedings of the National Academy of Sciences of the United States of America*, *112*(16), 5081–5086. https://doi.org/10.1073/pnas.1418034112

Jones, R. A., Williams, J. W., & Jackson, S. T. (2017). Vegetation history since the last glacial maximum in the Ozark highlands (USA): A new record from Cupola Pond, Missouri. *Quaternary Science Reviews*, *170*, 174–187. https://doi.org/10.1016/j.quascirev.2017.06.024

Kageyama, M., Merkel, U., Otto-Bliesner, B., Prange, M., Abe-Ouchi, A., Lohmann, G., et al. (2013). Climatic impacts of fresh water hosing under Last Glacial Maximum conditions: A multi-model study. *Climate of the Past*, *9*(2), 935–953. https://doi.org/10.5194/cp-9-935-2013

Kalnay, E., Kanamitsu, M., Kistler, R., Collins, W., Deaven, D., Gandin, L., et al. (1996). The NCEP/NCAR 40-year reanalysis project. *Bulletin of the American meteorological Society*, *77*(3), 437–471. https://doi.org/10.1175/1520-0477(1996)077<0437:TNYRP>2.0.CO;2

Kaufman, D., McKay, N., Routson, C., Erb, M., Davis, B., Heiri, O., et al. (2020). A global database of Holocene paleotemperature records. *Scientific Data*, *7*(1), 34.

Keigwin, L. D., Jones, G. A., Lehman, S. J., & Boyle, E. A. (1991). Deglacial meltwater discharge, North Atlantic deep circulation, and abrupt climate change. *Journal of Geophysical Research: Oceans*, *96*(C9), 16,811–16,826. https://doi.org/10.1029/91JC01624

Klinger, B. A., & Marotzke, J. (2000). Meridional heat transport by the subtropical cell. *Journal of Physical Oceanography*, *30*(4), 696–705. https://doi.org/10.1175/1520-0485(2000)030<0696:MHTBTS>2.0.CO;2

Kneller, M., & Peteet, D. (1993). Late-Quaternary climate in the Ridge and Valley of Virginia, U.S.A.: Changes in vegetation and depositional environment: A contribution to the 'North Atlantic seaboard programme' of IGCP-253, 'Termination of the Pleistocene. *Quaternary Science Reviews*, *12*(8), 613–628. https://doi.org/10.1016/0277-3791(93)90003-5

Krause, T. R., Russell, J. M., Zhang, R., Williams, J. W., & Jackson, S. T. (2019). Late Quaternary vegetation, climate, and fire history of the Southeast Atlantic Coastal Plain based on a 30,000-yr multi-proxy record from White Pond, South Carolina, USA. *Quaternary Research*, 1–20. https://doi.org/10.1017/qua.2018.95

Kumar, S., Kinter, J., Dirmeyer, P. A., Pan, Z. T., & Adams, J. (2013). Multidecadal climate variability and the "warming hole" in North America: Results from CMIP5 twentieth- and twenty-first-century climate simulations. *Journal of Climate*, *26*(11), 3511–3527.

Latham, R. E., & Ricklefs, R. E. (1993). Continental comparisons of temperate-zone tree species diversity. In R. E. Ricklefs & D. Schluter (Eds.), *Species diversity in ecological communities: Historical and geographical perspectives* (pp. 294–314). Chicago: University of Chicago Press.

Levesque, A. J., Cwynar, L. C., & Walker, I. R. (1997). Exceptionally steep north–south gradients in lake temperatures during the last deglaciation. *Nature*, *385*(6615), 423–426. https://doi.org/10.1038/385423a0

Liu, Z., Otto-Bliesner, B. L., He, F., Brady, E. C., Tomas, R., Clark, P. U., et al. (2009). Transient simulation of last deglaciation with a new mechanism for Bølling-Allerød warming. *Science*, *325*(5938), 310–314. https://doi.org/10.1126/science.1171041

Loomis, S. E., Russell, J. M., Ladd, B., Street-Perrott, F. A., & Sinninghe Damsté, J. S. (2012). Calibration and application of the branched GDGT temperature proxy on East African lake sediments. *Earth and Planetary Science Letters*, *357–358*, 277–288.

Lumibao, C. Y., Hoban, S. M., & McLachlan, J. (2017). Ice ages leave genetic diversity "hotspots" in Europe but not in Eastern North America. *Ecology Letters*, *20*(11), 1459–1468. https://doi.org/10.1111/ele.12853

McCreary, J. P., & Lu, P. (1994). Interaction between the subtropical and equatorial ocean circulations—The subtropical cell. *Journal of Physical Oceanography*, *24*(2), 466–497.

McGee, D., Moreno-Chamarro, E., Green, B., Marshall, J., Galbraith, E., & Bradtmiller, L. (2018). Hemispherically asymmetric trade wind changes as signatures of past ITCZ shifts. *Quaternary Science Reviews*, *180*, 214–228. https://doi.org/10.1016/j.quascirev.2017.11.020

McManus, J. F., Francois, R., Gherardi, J. M., Keigwin, L. D., & Brown-Leger, S. (2004). Collapse and rapid resumption of Atlantic meridional circulation linked to deglacial climate changes. *Nature*, *428*(6985), 834–837. https://doi.org/10.1038/nature02494

Meehl, G. A., Arblaster, J. M., & Branstator, G. (2012). Mechanisms contributing to the warming hole and the consequent US east-west differential of heat extremes. *Journal of Climate*, *25*(18), 6394–6408. https://doi.org/10.1175/JCLI-D-11-00655.1

Mix, A. C., Ruddiman, W. F., & McIntyre, A. (1986a). Late Quaternary paleoceanography of the tropical Atlantic, 2: Spatial variability of annual mean sea-surface temperatures, 0–20,000 years BP. *Paleoceanography*, *1*(3), 339–353. https://doi.org/10.1029/PA001i003p00339

Mix, A. C., Ruddiman, W. F., & McIntyre, A. (1986b). Late Quaternary paleoceanography of the tropical Atlantic. 1: Spatial variability of annual mean sea-surface temperatures, 0–20,000 years BP. *Paleoceanography*, *1*(1), 43–66. https://doi.org/10.1029/PA001i001p00043

North, G. R. (1984). The small ice cap instability in diffusive climate models. *Journal of the Atmospheric Sciences*, *41*(23), 3390–3395. https://doi.org/10.1175/1520-0469(1984)041<3390:TSICII>2.0.CO;2

North, G. R., Bell, T. L., Cahalan, R. F., & Moeng, F. J. (1982). Sampling errors in the estimate of empirical orthogonal functions. *Monthly Weather Review*, *110*(7), 699–706. https://doi.org/10.1175/1520-0493(1982)110<0699:SEITEO>2.0.CO;2

Okumura, Y. M., Deser, C., Hu, A., Timmermann, A., & Xie, S. P. (2009). North Pacific climate response to freshwater forcing in the subarctic North Atlantic: Oceanic and atmospheric pathways. *Journal of Climate*, *22*(6), 1424–1445. https://doi.org/10.1175/2008JCLI2511.1

Overpeck, J. T., Webb, T., & Prentice, I. C. (1985). Quantitative interpretation of fossil pollen spectra—Dissimilarity coefficients and the method of modern analogs. *Quaternary Research*, *23*(1), 87–108. https://doi.org/10.1016/0033-5894(85)90074-2

Pedro, J. B., Jochum, M., Buizert, C., He, F., Barker, S., & Rasmussen, S. O. (2018). Beyond the bipolar seesaw: Toward a process understanding of interhemispheric coupling. *Quaternary Science Reviews*, *192*, 27–46. https://doi.org/10.1016/j.quascirev.2018.05.005

Peterse, F., van der Meer, J., Schouten, S., Weijers, J. W. H., Fierer, N., Jackson, R. B., et al. (2012). Revised calibration of the MBT–CBT paleotemperature proxy based on branched tetraether membrane lipids in surface soils. *Geochimica et Cosmochimica Acta*, *96*, 215–229. https://doi.org/10.1016/j.gca.2012.08.011

Rasmussen, S. O., Andersen, K. K., Svensson, A. M., Steffensen, J. P., Vinther, B. M., Clausen, H. B., et al. (2006). A new Greenland ice core chronology for the last glacial termination. *Journal of Geophysical Research*, *111*, D06102. https://doi.org/10.1029/2005JD006079

Renssen, H., Goosse, H., Roche, D. M., & Seppa, H. (2018). The global hydroclimate response during the Younger Dryas event. *Quaternary Science Reviews*, *193*, 84–97. https://doi.org/10.1016/j.quascirev.2018.05.033

Rey, F., Gobet, E., van Leeuwen, J. F. N., Gilli, A., van Raden, U. J., Hafner, A., et al. (2017). Vegetational and agricultural dynamics at Burgaschisee (Swiss Plateau) recorded for 18,700 years by multi-proxy evidence from partly varved sediments. *Vegetation History and Archaeobotany*, *26*(6), 571–586. https://doi.org/10.1007/s00334-017-0635-x

Rodwell, M. J., Rowell, D. P., & Folland, C. K. (1999). Oceanic forcing of the wintertime North Atlantic Oscillation and European climate. *Nature*, *398*(6725), 320–323. https://doi.org/10.1038/18648

Rogers, J. C. (1990). Patterns of low frequency monthly sea level pressure variability (1899–1986) and associated wave cyclone frequencies. *Journal of Climate*, *3*(12), 1364–1379. https://doi.org/10.1175/1520-0442(1990)003<1364:POLFMS>2.0.CO;2

Ruhlemann, C., Mulitza, S., Muller, P. J., Wefer, G., & Zahn, R. (1999). Warming of the tropical Atlantic Ocean and slowdown of thermohaline circulation during the last deglaciation. *Nature*, *402*(6761), 511–514. https://doi.org/10.1038/990069

Russell, J. M., Hopmans, E. C., Loomis, S. E., Liang, J., & Sinninghe Damsté, J. S. (2018). Distributions of 5- and 6-methyl branched glycerol dialkyl glycerol tetraethers (brGDGTs) in East African lake sediment: Effects of temperature, pH, and new lacustrine paleotemperature calibrations. *Organic Geochemistry*, *117*, 56–69. https://doi.org/10.1016/j.orggeochem.2017.12.003

Sandel, B., Arge, L., Dalsgaard, B., Davies, R. G., Gaston, K. J., Sutherland, W. J., & Svenning, J. C. (2011). The influence of late Quaternary climate-change velocity on species endemism. *Science*, *334*(6056), 660–664. https://doi.org/10.1126/science.1210173

Shakun, J. D., & Carlson, A. E. (2010). A global perspective on Last Glacial Maximum to Holocene climate change. *Quaternary Science Reviews*, *29*(15–16), 1801–1816. https://doi.org/10.1016/j.quascirev.2010.03.016

Shuman, B., Webb, T. III, Bartlein, P., & Williams, J. W. (2002). The anatomy of a climatic oscillation: Vegetation change in eastern North America during the Younger Dryas chronozone. *Quaternary Science Reviews*, *21*(16–17), 1777–1791. https://doi.org/10.1016/S0277-3791(02)00030-6

Sinninghe Damsté, J. S., Rijpstra, W. I. C., Foesel, B. U., Huber, K. J., Overmann, J., Nakagawa, S., et al. (2018). An overview of the occurrence of ether- and ester-linked iso-diabolic acid membrane lipids in microbial cultures of the Acidobacteria: Implications for brGDGT paleoproxies for temperature and pH. *Organic Geochemistry*, *124*, 63–76. https://doi.org/10.1016/j.orggeochem.2018.07.006

Stocker, T. F. (1998). Climate change—The seesaw effect. *Science*, *282*(5386), 61–62. https://doi.org/10.1126/science.282.5386.61
Stocker, T. F., Wright, D. G., & Mysak, L. A. (1992). A zonally averaged, coupled ocean-atmosphere model for paleoclimate studies. *Journal of Climate*, *5*(8), 773–797. https://doi.org/10.1175/1520-0442(1992)005<0773:AZACOA>2.0.CO;2
Talbot, M. R., Filippi, M. L., Jensen, N. B., & Tiercelin, J. J. (2007). An abrupt change in the African monsoon at the end of the Younger Dryas. *Geochemistry Geophysics Geosystems*, *8*, Q3005. https://doi.org/10.1029/2006GC001465
Ter Braak, C. J. (1987). Unimodal models to relate species to environment, Wageningen University.
Ter Braak, C. J., & Prentice, I. C. (1988). A theory of gradient analysis. In *Advances in Ecological Research* (Vol. 18, pp. 271–317). London: Academic Press. https://doi.org/10.1016/S0065-2504(08)60183-X
Ter Braak, C. J. F., & Juggins, S. (1993). Weighted averaging partial least squares regression (WA-PLS): An improved method for reconstructing environmental variables from species assemblages. In H. van Dam (Ed.), *Twelfth international diatom symposium: Proceedings of the twelfth international diatom symposium, Renesse, The Netherlands, 30 August–5 September 1992* (pp. 485–502). Netherlands, Dordrecht: Springer.
Ter Braak, C. J. F., Juggins, S., Birks, H. J. B., & Vandervoet, H. (1993). Weighted Averaging Partial Least-Squares regression (WA-PLS): Definition and comparison with other methods for species-environment calibration. *N-Holland Stat Prob*, *6*, 525–560.
Thompson, R. S., Anderson, K. H., & Bartlein, P. J. (1999a). Atlas of relations between climatic parameters and distributions of important trees and shrubs in North America-Hardwoods. In *U.S. Department of the Interior* (p. 423). Denver, CO: U.S. Department of the Interior, U.S. Geological Survey.
Thompson, R. S., Anderson, K. H., & Bartlein, P. J. (1999b). Atlas of relations between climatic parameters and distributions of important trees and shrubs in North America—Introduction and conifers. In *U.S. Department of the Interior* (p. 269). Denver, CO: U.S. Department of the Interior, U.S. Geological Survey.
Tierney, J. E., Zhu, J., King, J., Malevich, S. B., Hakim, G. J., & Poulsen, C. J. (2020). Glacial cooling and climate sensitivity revisited. *Nature*, *584*(7822), 569–573. https://doi.org/10.1038/s41586-020-2617-x
Toomey, M. R., Korty, R. L., Donnelly, J. P., van Hengstum, P. J., & Curry, W. B. (2017). Increased hurricane frequency near Florida during Younger Dryas Atlantic Meridional Overturning Circulation slowdown. *Geology*, *45*(11), 1047–1050. https://doi.org/10.1130/G39270.1
van Loon, H., & Rogers, J. C. (1978). The seesaw in winter temperatures between Greenland and northern Europe. Part I: General description. *Monthly Weather Review*, *106*(3), 296–310. https://doi.org/10.1175/1520-0493(1978)106<0296:TSIWTB>2.0.CO;2
Walker, G. T., & Bliss, E. W. (1932). World weather V. In *Memoirs of the Royal Meteorological Society* (pp. 53–84). Stanford, London.
Wallace, J. M., & Gutzler, D. S. (1981). Teleconnections in the geopotential height field during the Northern Hemisphere winter. *Monthly Weather Review*, *109*(4), 784–812. https://doi.org/10.1175/1520-0493(1981)109<0784:TITGHF>2.0.CO;2
Wang, C. Z. (2002). Atlantic climate variability and its associated atmospheric circulation cells. *Journal of Climate*, *15*(13), 1516–1536. https://doi.org/10.1175/1520-0442(2002)015<1516:ACVAIA>2.0.CO;2
Wang, Y., Goring, S. J., & McGuire, J. L. (2019). Bayesian ages for pollen records since the last glaciation in North America. *Scientific Data*, *6*, 8.
Watson, B. I., Williams, J. W., Russell, J. M., Jackson, S. T., Shane, L., & Lowell, T. V. (2018). Temperature variations in the southern Great Lakes during the last deglaciation: Comparison between pollen and GDGT proxies. *Quaternary Science Reviews*, *182*, 78–92. https://doi.org/10.1016/j.quascirev.2017.12.011
Watts, W. A. (1980b). The late Quaternary vegetation history of the southeastern United States. *Annual Review of Ecology and Systematics*, *11*(1), 387–409. https://doi.org/10.1146/annurev.es.11.110180.002131
Weijers, J. W. H., Schouten, S., van den Donker, J. C., Hopmans, E. C., & Sinninghe Damsté, J. S. (2007). Environmental controls on bacterial tetraether membrane lipid distribution in soils. *Geochimica et Cosmochimica Acta*, *71*(3), 703–713. https://doi.org/10.1016/j.gca.2006.10.003
Whitmore, J., Gajewski, K., Sawada, M., Williams, J. W., Shuman, B., Bartlein, P. J., et al. (2005). Modern pollen data from North America and Greenland for multi-scale paleoenvironmental applications. *Quaternary Science Reviews*, *24*(16–17), 1828–1848. https://doi.org/10.1016/j.quascirev.2005.03.005
Williams, J., & Shuman, B. (2008). Obtaining accurate and precise environmental reconstructions from the modern analog technique and North American surface pollen dataset. *Quaternary Science Reviews*, *27*(7–8), 669–687. https://doi.org/10.1016/j.quascirev.2008.01.004
Williams, J. W., Shuman, B., Bartlein, P. J., Whitmore, J., Gajewski, K., Sawada, M., et al. (2006). *An Atlas of Pollen–Vegetation–Climate Relationships for the United States and Canada* (p. 293). Dallas, TX: American Association of Stratigraphic Palynologists Foundation.
Williams, J. W., & Burke, K. D. (2019). Past abrupt changes in climate and terrestrial ecosystems. In T. Lovejoy, & L. Hannah (Eds.), *Climate Change and Biodiversity: Transforming the Biosphere* (pp. 128–141). New Haven, CT: Yale University Press.
Williams, J. W., Grimm, E. C., Blois, J. L., Charles, D. F., Davis, E. B., Goring, S. J., et al. (2018). The Neotoma Paleoecology Database, a multiproxy, international, community-curated data resource. *Quaternary Research*, *89*(1), 156–177. https://doi.org/10.1017/qua.2017.105
Ziegler, M., Nurnberg, D., Karas, C., Tiedemann, R., & Lourens, L. J. (2008). Persistent summer expansion of the Atlantic Warm Pool during glacial abrupt cold events. *Nature Geoscience*, *1*(9), 601–605.

References From the Supporting Information

Hussey, T. C. (1993). A 20,000-year history of vegetation and climate at Clear Pond, northeastern South Carolina, University of Maine.
Kaufman, D., McKay, N., Routson, C., Erb, M., Datwyler, C., Sommer, P. S., et al. (2020a). Holocene global mean surface temperature, a multi-method reconstruction approach. *Scientific Data*, *7*(1), 13.
Kneller, M., & Peteet, D. (1999). Late-glacial to early Holocene climate changes from a central Appalachian pollen and macrofossil record. *Quaternary Research*, *51*(2), 133–147. https://doi.org/10.1006/qres.1998.2026
Reimer, P. J., Bard, E., Bayliss, A., Beck, J. W., Blackwell, P. G., Ramsey, C. B., et al. (2013). IntCal13 and Marine13 radiocarbon age calibration curves 0–50,000 years cal BP.
Watts, W. A. (1975). A late Quaternary record of vegetation from Lake Annie, south-central Florida. *Geology*, *3*(6), 344–346. https://doi.org/10.1130/0091-7613(1975)3<344:ALQROV>2.0.CO;2
Watts, W. A. (1980a). Late-Quaternary vegetation history at White Pond on the inner coastal-plain of South Carolina. *Quaternary Research*, *13*(2), 187–199. https://doi.org/10.1016/0033-5894(80)90028-9